JOURNAL OF CHEMICAL & ENGINEERING DATA

ARTICLE

pubs.acs.org/jced

Removal of Bromocresol Green from Aqueous Solution via Adsorption on *Ziziphus nummularia* as a New, Natural, and Low-Cost Adsorbent: Kinetic and Thermodynamic Study of Removal Process

A. Shokrollahi,* A. Alizadeh, Z. Malekhosseini, and M. Ranjbar

Department of Chemistry, Yasouj University 75918-74831, Yasouj, Iran

ABSTRACT: In this study *Ziziphus nummularia* (ZPN) as a good, available and inexpensive adsorbent has been introduced and used for the removal of Bromocresol Green (BCG) from several water solutions successfully. The effect of various parameters such as pH, dye concentration, amount of adsorbent, size of adsorbent particles, and contact time on removal processing was investigated. To investigate the mechanism of adsorption, several kinetic models were tested including Lagergren, pseudosecond-order, particle diffusion, film diffusion, and Elovich models. Adsorption isothermal data could be interpreted by the Langmuir, Freundlich, Tempkin, and Dubinin−Rudushkevich (DR) isotherm models. Thermodynamic parameters like free energy (ΔG), enthalpy (ΔH), and entropy (ΔS) of the system were calculated.

INTRODUCTION

Dyes are widely used in industries such as textiles, rubber, paper, plastics, cosmetics, and so forth. Dye pollutants in our wastewaters are a major source of environmental contamination. Dyes are ordered in three broad classes:

(1) Anionic: direct, acid, and reactive dyes;
(2) Cationic: basic dyes;
(3) Nonionic: disperse dyes.

Bromocresol Green (BCG) is a dye of the triphenylmethane (anionic) family which is used as a pH indicator and as a tracking dye for DNA agarose gel electrophoresis. In addition, it is used in the weaving industry like cotton and linen. BCG can be used in its free acid form (light brown solid) or as a sodium salt (dark green solid). Many of the industrial dyes are toxic, carcinogenic, and mutagenic, causing skin sensitivity and eye diseases.[1−5] Therefore, their removal from wastewater is of great interest. Dyes usually have a synthetic origin and complex aromatic molecular structures, which make them more stable and biodegradation more difficult. Dyes even in low concentrations affect the aquatic life and food web. Thus, it is important to remove dyes from effluents before they are mixed up with unpolluted natural water bodies. Many investigators have studied different techniques for removal of colored dye from wastewater, and one of the powerful and convenient treatment processes is adsorption. Activated carbon is the most widely used adsorbent for this purpose, it is capable of adsorbing many dyes with a high adsorption capacity, but it is expensive and costs of regeneration are high because desorption of the dye molecules is not easily achieved. Nowadays, a number of low-cost, commercially available adsorbents have been tried for dye removal. Adsorbents used include agricultural solid wastes such as: fly ash, coal-burning industries, saw dust, wood, banana pith, pine saw dust, palm seed and etc.[6−11] In general, these carbons are efficient in the adsorption of both organic and inorganic as the commercial activated carbons.

In the present investigation, *Ziziphus nummularia* (ZPN) is used as an adsorbent for the first time. ZPN (Scheme 1), also called Jharber (Hindi), is a species of *Ziziphus* native to the desert of south Iran (where it is called ramilak in Persian), southeastern Pakistan, and western India. It is a shrub up to 2 m high, branching to form a thicket. The plant is commonly found in agricultural fields. The leaves are collected, dried, and stored. The dried leaves, called Pala, are used as fodder for goats and cows. The fruits are eaten and when dried are used medicinally in ayruveda. The roots are used locally to prepare wine. The dried spiny twigs are collected in heaps for fencing.[12] The ZPN used in this study were collected from Kohgilluye and Noorabad Mamassani in the south of Iran.

Scheme 1. *Ziziphus nummularia*

The purpose of this work was to introduce ZPN as a new and high quality adsorbent. It also aimed at studying the removal of BCG as a typical dye from water, by adsorbing via batch system.

EXPERIMENTAL SECTION

Materials. BCG with the molecular formula $C_{12}H_{14}Br_4O_5S$ was obtained from Columbus Chemical Industries, Inc., Columbus,

Received: March 31, 2011
Accepted: July 19, 2011
Published: August 31, 2011

dx.doi.org/10.1021/je200311y | *J. Chem. Eng. Data* 2011, 56, 3738–3746

Scheme 2. Chemical Structure of BCG

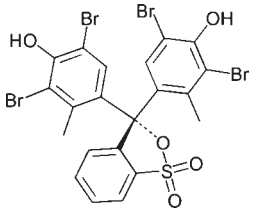

WI 53925 (Scheme 2); HCl and NaOH were obtained from Merck Co. (Darmstadt, Germany). The stock solution and all other solutions of BCG were prepared in double-distilled water. Bashar River water, tap water, and mineral water samples were investigated.

Apparatus. The concentration of BCG in each aqueous solution was measured with a Jasco model V-570 spectrophotometer (Jasco Co., Hachioji, Tokyo, Japan) by measuring the absorbance at λ_{max} of 442 nm. The pH solution of the dye was measured with a pH meter model 827 (Metrohm Co., Herisau, Switzerland), and the pH adjustments were made using dilute NaOH and HCl solutions. Scanning electron microscopy (SEM) micrographs using a scanning electron microscope Leica/Cambridge S-360 were studied. An Fourier transform infrared (FT-IR) analysis for ZPN was performed using a KBr disk by a Shimadzu FTIR-8300 spectrophotometer (Shimadzu Co. Tokyo, Japan). A model 794 Metrohm Basic titrino was attached to an extension combined glass-calomel electrode mounted in an air-protected, sealed, thermostatted jacketed cell maintained at 25.0 ± 0.1 °C by circulating water, from a constant-temperature bath, Fisherbrand model FBH604, Lauda, Germany, equipped with a stirrer and a 10.000 mL capacity Metrohm piston buret. The pH meter-electrode system was calibrated to read $-\log(H^+)$.

Potentiometric Equilibrium Measurements. The details are described in refs 29 to 32. The concentration of BCG was $2.5 \cdot 10^{-3}$ M, for the potentiometric pH titration. A standard carbonate-free NaOH solution (0.10591) was used in titration. The ionic strength was adjusted to 0.1 M with $NaNO_3$. Before an experimental point (pH) was measured, sufficient time was given to establish equilibrium. Protonation constants of BCG were evaluated using the BEST program,[33] and the corresponding distribution diagrams were depicted using Hyss2009 as a new version of Hyss2006 program.[34] The value of $K_W = [H^+][OH^-]$ used in the study was the same as that of our previous works.[29−31]

Preparation of Adsorbent. The adsorbent materials were collected and washed with distilled water to remove dirt and impurities and dried in the sun, and then for acid treatment it was mixed with concentrated hydrochloric acid (37 %) at room temperature for 24 h. The sample was then washed several times with distilled water, filtrated, dried at 120 °C for 1 h, and sieved to the particle sizes through 10-50 mesh. The product obtained was stored in a closed container for further tests.[13]

FT-IR Analysis. To determine which functional groups were responsible for dye adsorption, an FT-IR analysis for ZPN was performed using a KBr disk. The spectra (Figure 1) display a number of adsorption peaks. The FT-IR of the ZPN showed adsorption peaks around 3407 cm^{-1}, which is indicative of the existence of bonded hydroxyl groups, and the peak observed at 2854 cm^{-1} can be assigned to the C−H group. The peak observed at 1743 cm^{-1} is due to CO, and the peak at 1605 cm^{-1}

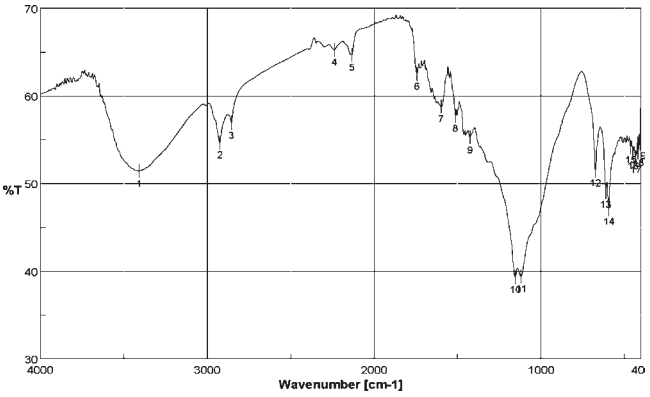

Figure 1. FT-IR of ZPN.

is due to the C═C stretching that can be attributed to the aromatic C−C bond. The peak around 1424 cm^{-1} is due to the symmetric bending of CH_3. The peaks around 2854 cm^{-1} and 2924 cm^{-1} can be assigned to the CHO groups. The adsorption band at 1590 cm^{-1} is ascribed to the NH.[14−16]

Scanning Electron Microscopy (SEM). SEM is a widely used technique for the determination of morphology and size distribution of prepared particles in the scales of micro to nano range. Figures 2a,b show the SEM micrographs of adsorbent before and after dye adsorption, respectively. It shows that the adsorbent possesses a surface morphology with pores of different sizes; these pores are useful for dye adsorption.[7]

Adsorption Studies. Batch mode adsorption method was followed. Batch experiments were conducted to observe the effect of pH, temperature, particle size, amount of adsorbent, initial concentration of dye, contact time, and so forth. For equilibrium adsorption studies, a known amount of adsorbent was equilibrated with desired dye solution at room temperature for definite time periods. At the end of the predetermined time intervals, the adsorbent was removed by simple filtration. The filtrate was analyzed for the residual (unadsorbed) BCG, spectrophotometrically. For kinetic studies experiments were done with fixed carbon with varying contact times. Kinetic studies were also carried out at different adsorbate concentrations. Adsorption isotherms were carried out at condition equilibrium for concentrations of dye at a fixed pH (pH = 2). The amount of dye adsorption by ZPN, q_e ($mg \cdot g^{-1}$), was obtained as follows:

$$q_e = \frac{(C_o - C_e) \cdot V}{W} \quad (1)$$

where C_0 and C_e are the initial and equilibrium concentration of dye in solution, respectively, W is the weight of adsorbent (g), and V is the solution volume.[16,17]

RESULTS AND DISCUSSION

Protonation Studies. In this section, the fully protonated forms of BCG were titrated with a standard NaOH solution to obtain the protonation constants. The protonation constants were calculated by fitting the pH/volume data to the BEST program. It is obvious that two groups on BCG (L) are protonated at pH 2 and < 2, leading to the formation of LH_2. At pH 3.6 and pH > 7, the abundance of species LH^- and L^{2-} are respectively reached to the maximum. So at higher pH, gradually

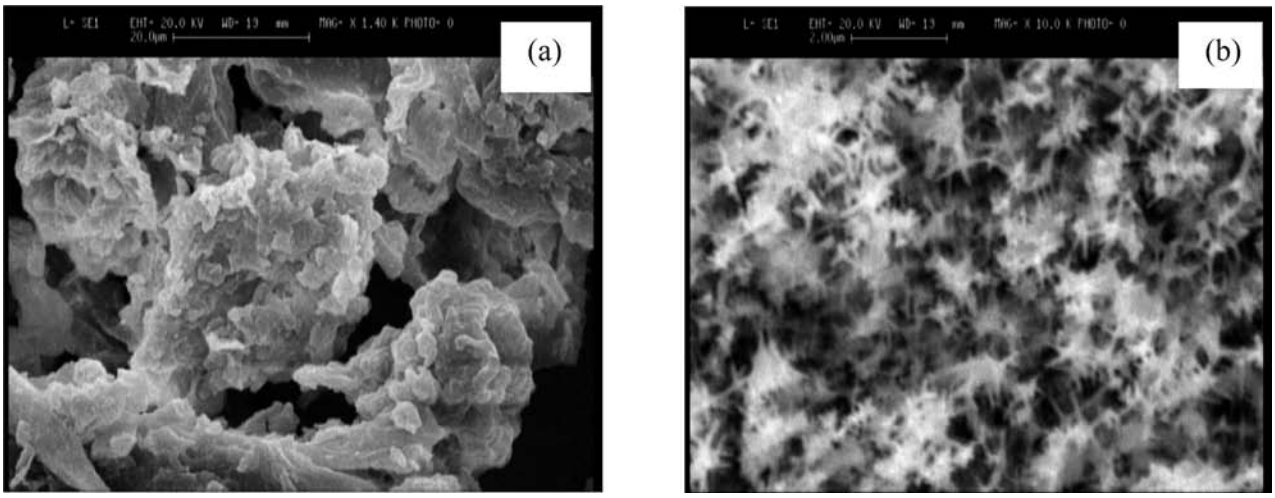

Figure 2. SEM micrographs of adsorbent samples before (a) and after (b) dye adsorption.

the protons are loosed, and the various forms including LH^- and L^{2-} are obtained.

Effect of System pH on BCG Adsorption. The pH of the system is very effective on the capacity of adsorbate molecule presumably due to its influence on the surface properties of the adsorbent, ionization, and dissociation of the adsorbate molecule. BCG removal was studied as a function of pH at a fixed concentration and adsorbent dosage. The percentage of BCG adsorption decreases while pH increases from 1.0 to 2.0 and decreases while pH declines from 2.0 to 6.0. In pH = 1, due to the excess of proton, the charge of BCG (anionic dye) is positive, and the electrostatic attraction in comparison to pH = 2 is less. In pH = 2, the positive charge of BCG decreases, and BCG interaction with adsorbent surface increases. In pH > 2 BCG has a negative charge, and electrostatic repulsion decreases attraction.[11,18] Therefore, pH = 2 was selected as an optimum parameter. This observation is confirmed by the obtained results from the potentiometric study.

Effect of Adsorbent Amount. To study the variation in adsorption based on the amount of the adsorbent material, in the conditions of dye concentration (50 $mg \cdot L^{-1}$) and pH = 2, the various amounts [(0.04 to 0.8) g] of ZPN were selected. With increasing the amount of adsorbent to 0.4 g, the adsorption capacity increases, but there is no change when the amount of adsorbent exceeds 0.4 g. An increase in the adsorption with a high dosage of the adsorbent is due to an increased adsorbent surface area of mesopores and the availability of more adsorption sites.[19]

Effect of Particle Size. To observe the effect of particle size of adsorbent, six different sizes, namely, 10, 10-20, 20-30, 30-40, 40-50, and 50 mesh of ZPN, were investigated. By decreasing the size of adsorbent material, the percentage adsorption of the dye increases. This may be due to the increase in surface area of the adsorbent material with the decrease in its size; thus the mesh 30-50 was selected for further experiments.[20,21]

Effect of Time of Contact. The relation between the adsorption of BCG and contact time was investigated to identify the rate of dye removal. The adsorption increases with increasing contact time. Then, the rate of adsorption becomes slow. The rapid adsorption at the initial contact time is due to the availability of the positively charged surface of adsorbent, which leads to fast electrostatic adsorption of the anionic BCG from the solution at pH = 2. The equilibrium was found to be nearly 8 min for 50 $mg \cdot L^{-1}$.[14]

Adsorption Kinetics. The rate and mechanism of the adsorption process can be elucidated based on kinetics studies. Dye adsorption on solid surface may be explained by two distinct mechanisms:

(1) An initial rapid binding of dye molecules on the adsorbent surface;
(2) Relatively slow intraparticle diffusion.

To analyze the adsorption kinetics of dye, the first-order, the pseudosecond-order, and intraparticle or film diffusion models were applied to data obtained from the experiments.[7,22]

Pseudofirst-Order Kinetics. Pseudofirst-order kinetics is described by the following equation:

$$\frac{dq_t}{q_t} = K_1(q_e - q_t) \tag{2}$$

where q_e and q_t are the amounts ($mg \cdot g^{-1}$) of adsorbate at equilibrium and at time t (s), respectively, and k_1 is the constant rate (s^{-1}). Integrating eq 2 at the boundary of $q_t = 0$ at $t = 0$ and $q_t = q_t$ at $t = t$, the equation can be converted linearly into the following equation:[23]

$$\log(q_e - q_t) = \log q_e - \frac{K_1}{2.303} \cdot t \tag{3}$$

Plotting the values of log $(q_e - q_t)$ versus t gives a linear relationship from which k_1 and q_e can be determined from the slope and intercept of Figure 3, respectively. If the intercept (calculated q_e) does not equal experimental q_e, then the reaction is not likely to be a first-order reaction, even though this plot has a high correlation coefficient with the experimental data in Table 1. The calculated q_e values are too low compared with experimental q_e values that indicate that the adsorption of BCG onto ZPN is not a first-order reaction.[14]

Pseudosecond-Order Kinetics. The pseudosecond-order model is represented by the following differential equation:

$$\frac{dq_t}{dt} = K_2(q_e - q_t)^2 \tag{4}$$

where K_2 ($g \cdot mg^{-1} \cdot min^{-1}$) is the second-order rate constant of adsorption. Integration of eq 4 for the boundary conditions $q_t = 0$

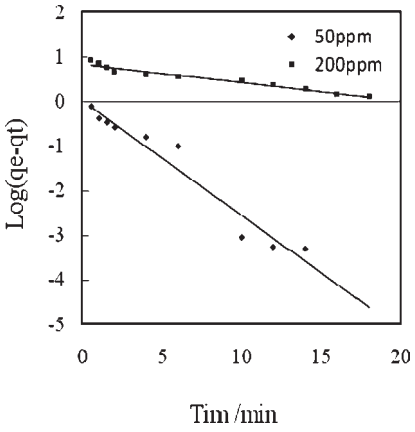

Figure 3. Pseudofirst-order kinetic model plot for the adsorption of BCG at concentrations of (50 and 200) mg·L^{-1}: ZPN (0.4 g) at pH = 2.

Table 1. Adsorption Kinetics Parameters for the Adsorption of BCG Concentration, (50 and 200) mg·L^{-1}: ZPN (0.4 g) at pH = 2

		initial BCG concentration (mg·L^{-1})	
model	parameters	50	200
first-order kinetic	k_1	0.60	0.094
	$q_{e(calc)}$	1.03	6.839
	R^2	0.956	0.965
second-orderkinetic	k_2	1.83	0.062
	$q_{e(calc)}$	6.25	24.39
	R^2	1.00	0.997
intraparticle diffusion	k_{diff}	0.134	1.557
	C	5.668	16.77
	R^2	0.879	0.941
q_e(exp)		6.197	24.64

to $q_t = q_t$ at $t = 0$ to $t = t$ is simplified, as it can be rearranged and linearized to obtain:

$$\frac{t}{q_t} = \frac{1}{K_2 \cdot q_e^2} + \frac{1}{q_e}(t) \qquad (5)$$

Plot the values of t/q_t versus t to give a linear relationship which K_2 and q_e can be determined from intercept and slope, respectively (Figure 4). The calculated q_e values are almost near experimental q_e values and the correlation coefficient R^2 is high, which indicates that the adsorption of BCG on ZPN is a second-order reaction[24] (Table 1).

Intraparticle Diffusion. Adsorption is a multistep process involving the transport of the adsorbate (dye) molecules from the aqueous phase to the surface of the solid (ZPN) particles then followed by diffusion of the solute molecules into the pore interior[14] (Figure 5). The successive steps in the adsorption of an organic/inorganic compound by an adsorbent are:

(1) Transport of the ingoing adsorbate to the external surface of the adsorbent (film diffusion);
(2) Transport of the adsorbate within the pores of the adsorbent except for a small amount of adsorption, which occurs on the external surface (particle diffusion);

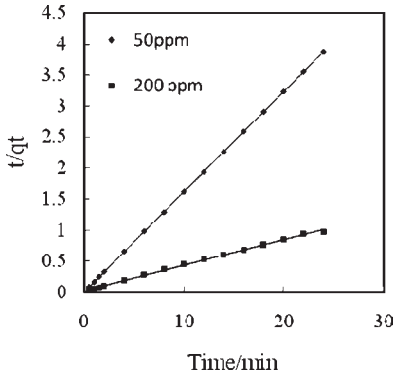

Figure 4. Pseudosecond-order kinetic model plot for the adsorption of BCG at concentrations of (50 and 200) mg·L^{-1}: ZPN (0.4 g) at pH = 2.

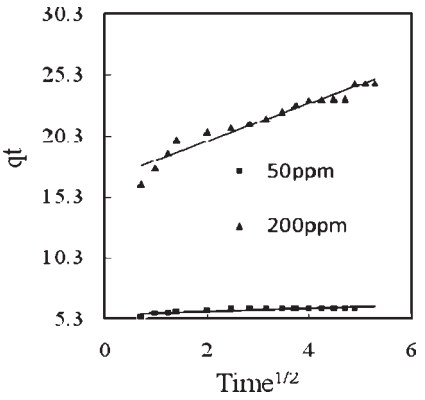

Figure 5. Intraparticle diffusion model plot for the adsorption of BCG at concentrations of (50 and 200) mg·L^{-1}: ZPN (0.4 g) at pH = 2.

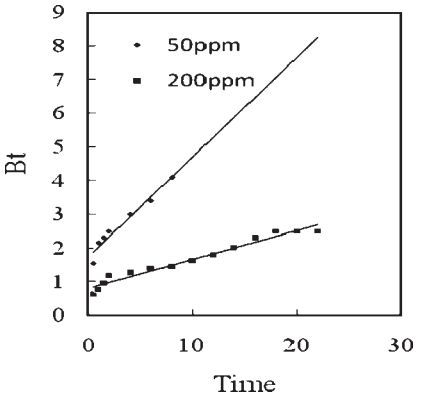

Figure 6. B_t vs time plots for the adsorption of BCG at concentrations of (50 and 200) mg·L^{-1}: ZPN (0.4 g) at pH = 2.

(3) Adsorption of the ingoing adsorbate on the interior surface of the adsorbent.[11]

Of the above three steps, the third step is considered to be very fast; thus, it cannot be treated as the rate-limiting step. The remaining two steps provide the following information:

(1) External transport > internal transport, where the rate is governed by particle diffusion;
(2) External transport < internal transport, where the rate is governed by film diffusion;

dx.doi.org/10.1021/je200311y |J. Chem. Eng. Data 2011, 56, 3738–3746

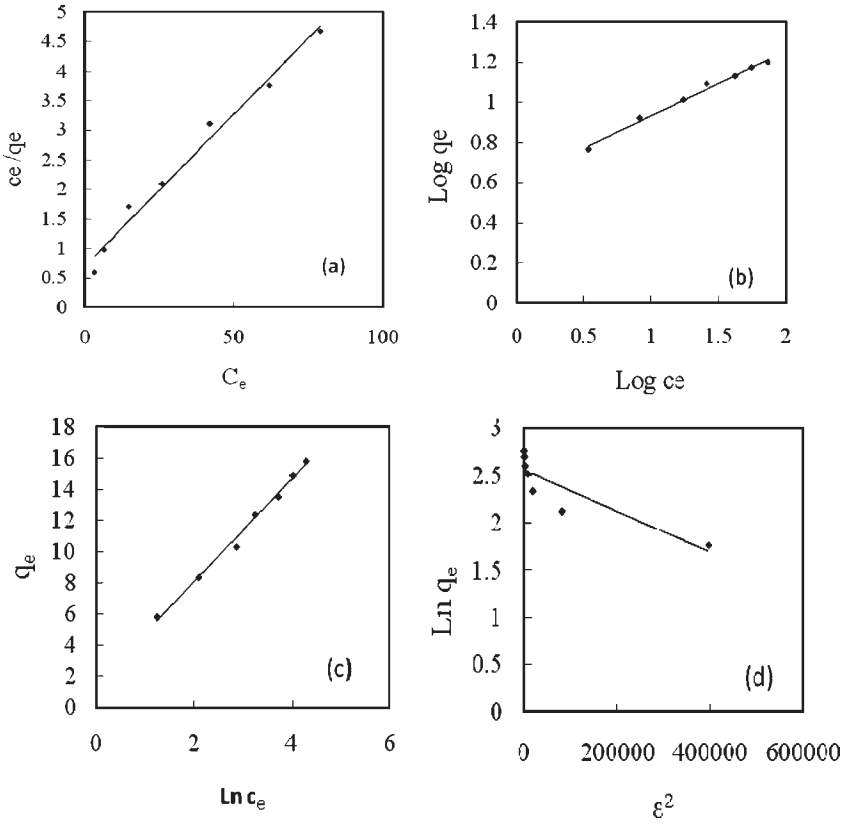

Figure 7. Langmuir (a), Freundlich (b), Tempkin (c), DR, (d) isotherm models plot for the adsorption of BCG at concentrations of (50 to 200) mg·L^{-1}: ZPN (0.4 g), pH = 2.

(3) External transport ≈ internal transport, which indicates that the transport of adsorbate to the boundary may not be possible at a significant rate; thus, the formation of a liquid film surrounding the adsorbent particles takes place through the proper concentration gradient.[23] A quantitative treatment of the adsorption dynamics was done via determining the fractional attainment F, of equilibrium at time t using the following expressions:[21]

$$F = 1 - \frac{6}{\pi^2}\sum_{1}^{\infty}\left(\frac{1}{n^2}\right)\exp(-n^2 B_t) \quad (6)$$

$$F = \frac{Q_t}{Q_\infty} \qquad B = \frac{\pi^2 D_i}{r_o{}^2} = \text{timeconstant} \quad (7)$$

where Q_t and Q_∞ are amounts adsorbed after the time of t and after infinite time, respectively. F is the fractional attainment of equilibrium at the time of t, D_i the effective diffusion coefficient of adsorbates in adsorbent phase, r the radius of adsorbent particle, and n is Freundlich constant of the adsorbate.[25] The film diffusion and particle diffusion adsorption rate were determined based on the plot B_t as a function of time through the Reichenberg table (Figure 6). If the obtained straight lines do not pass through origin, it reveals that the rate-determining process is film diffusion.[17]

Adsorption Isotherms. The successful application of the adsorption technique demands studies based on various adsorption isotherm models. Equilibrium relationships between adsorbent and adsorbate are described by adsorption isotherms.[21] The applicability of the isotherm equations is compared through interpreting the correlation coefficient R^2. The isotherm studies were performed by varying the initial BCG concentration from (50 to 200) mg·L^{-1} at pH = 2 which was adjusted using HCl or NaOH before adding of ZPN and maintained throughout the experiment.[26] After 8 min, the reaction mixture was analyzed for the residual BCG concentration. Next the Freundlich, Langmuir, Tempkin, and DR isothermal models were applied to the experimental data.[14]

Table 2. Comparison of the Coefficient Isotherm Parameters for BCG Adsorption onto ZPN (0.4 g)

Freundlich	Langmuir	Tempkin	DR
R^2 = 0.989	R^2 = 0.983	R^2= 0.992	R^2= 0.775
n = 3.090	Q_m = 19.61	K_1 = 3.279	Q_m = 12.89
K_f = 4.074	b = 0.073	K_2 = 1.570	$K_f = 2\cdot10^{-6}$
	R_L = 0.215		

Langmuir Isotherm. The Langmuir equation, which is valid for monolayer adsorption onto a completely homogeneous surface with a finite number of identical sites and with negligible interaction between adsorbed molecules, is represented in the linear form as follows:

$$\frac{C_e}{q_e} = \frac{1}{bQ_m} + \frac{C_e}{Q_m} \quad (8)$$

dx.doi.org/10.1021/je200311y |J. Chem. Eng. Data 2011, 56, 3738–3746

Table 3. Thermodynamic Parameters

initial concentration		temperature (K)					
$mg \cdot L^{-1}$	parameter	283	293	303	313	323	333
50	$\Delta G°$ ($kJ \cdot mol^{-1}$)	−5.41	−6.70	−7.85	−8.25	−8.56	−9.04
150		0.095	−0.63	−1.35	−2.07	−2.79	−3.52

initial concentration	$\Delta S°$	$\Delta H°$	E_a	
$mg \cdot L^{-1}$	$J \cdot mol^{-1} \cdot K^{-1}$	$kJ \cdot mol^{-1}$	$kJ \cdot mol^{-1}$	S^*
50	83.81	18.31	17.40	$6.4 \cdot 10^{-5}$
150	72.21	20.53	12.04	$2.9 \cdot 10^{-3}$

where b is the Langmuir adsorption constant ($L \cdot mg^{-1}$) and Q_m is the theoretical maximum adsorption capacity ($mg \cdot g^{-1}$). Figure 7a shows the Langmuir (c_e/q_e vs c_e) plots for the adsorption of BCG. The value of Q_m, the b constant, R_L, and the correlation coefficients for the Langmuir isotherm are presented in Table 2. The essential features of the Langmuir isotherm may be expressed in terms of equilibrium parameter R_L, which is a dimensionless constant referred to as a separation factor or equilibrium parameter.[24]

$$R_L = \frac{1}{1 + bC_o}$$

where C_o is the initial concentration and b is the constant related to the energy of adsorption (Langmuir constant).[10] The values of R_L indicate the type of isotherm to be irreversible ($R_L = 0$), favorable ($0 < R_L < 1$), linear ($R_L = 1$) or unfavorable ($R_L > 1$). Value of separation for adsorbent is found to be less than unity, confirming thereby the favorable adsorption process.[27]

Freundlich Model. Freundlich model assumes a heterogeneous adsorption surface with sites that have different energies of adsorption and are not equally available. The Freundlich equation is more widely used but provides no information on the monolayer adsorption capacity in contrast to the Langmuir model.[15] The Freundlich isotherm equation is:

$$q_e = K_f C^{1/n} \quad \text{(nonlinearform)} \tag{9}$$

$$\log q_e = \log K_f + \left(\frac{1}{n}\right) \log C_e \quad \text{(linearform)} \tag{10}$$

where q_e is the amount of adsorbate ($mg \cdot g^{-1}$), c_e is the equilibrium or residual concentration (mg^{-1}) of BCG dye in solution, and k and $1/n$ are empirical Freundlich constants indicating the adsorption capacity of adsorbent and intensity of adsorption ($mg \cdot g^{-1}$), respectively.[8] The linear plot of log q_e versus log c_e showed that adsorption followed the Freundlich adsorption isotherm model. Figure 7b and Table 2 show the Freundlich adsorption isotherm constant and correlation coefficient. The value of $1/n$ for the Freundlich isotherm was found to lie between zero and one, indicating that BCG is favorably adsorbed by ZPN.[24]

Tempkin Isotherm. The derivation of Tempkin isotherm assumes that the fall in the heat of adsorption is linear rather than logarithmic as implied in the Freundlich equation. The heat of adsorption of all of the molecules in the layer would decrease linearly with coverage due to adsorbate/adsorbate interaction.[28] The linear form of the Tempkin isotherm can be expressed as:

$$q_e = K_1 \ln K_2 + K_1 \ln C_e \tag{11}$$

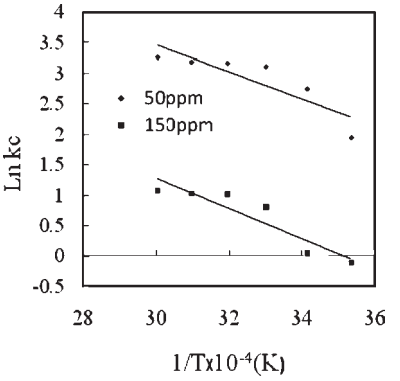

Figure 8. van't Hoff plots for the adsorption of BCG at concentrations of (50 and 150) $mg \cdot L^{-1}$ onto ZPN (0.4 g).

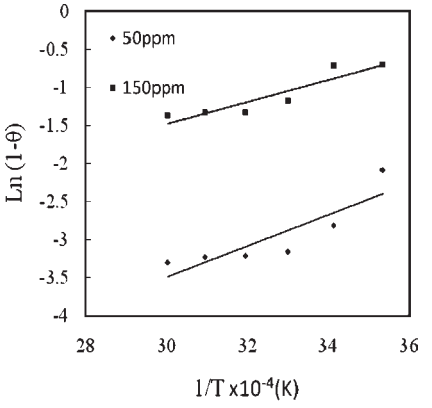

Figure 9. Plots of $\ln(1 - \theta)$ versus $1/T$ for the adsorption of BCG at concentrations of (50 and 150) $mg \cdot L^{-1}$ onto ZPN (0.4 g).

Table 4. Removal of BCG from Real Samples

	BCG added	
sample	$mg \cdot L^{-1}$	% removal
Bashar River water	50	97.85
tap water	50	96.21
mineral water	50	96.45

C_e = concentration of the dye at equilibrium ($mg \cdot L^{-1}$), q_e = amount of dye adsorbed at equilibrium ($mg \cdot g^{-1}$), K_1 (RT/b) is

Table 5. Adsorption Characteristics for the Removal of Dyes by Different Adsorbents

adsorbent	adsorbate	adsorption capacity mg·g^{-1}	concentration	contact time	ref
AC[a]-charcoal	Acid Blue	100.90	10−25 mg·dm^{-3}	21 days	35
blast furnace sludge	Ethyl Orange	1.30	25−200 mg·L^{-1}	180 min	36
zeolite	Basic dye Maxilon	14.91	20−200 mg·dm^{-3}	4−10 days	37
coal	Metomega Chrome orange	0.77	10 mg·L^{-1}	80 min	38
sugar cane dust	Basic Violet 10	3.24	12 mg·L^{-1}	30 min	39
cane pith	Basic Red 22	941.70	50−600 mg·dm^{-3}	5 days	40
alumina	Alizarin Red s	0.69	25 mg·L^{-1}	35 min	41
silica gel	Methyl Orange	47.17	100 mg·L^{-1}	20 min	42
ZPN	BCG	6.21	50 mg·L^{-1}	8 min	proposed method

[a] Activated.

related to the heat of adsorption, and K_2 is the equilibrium binding constant (L·mg^{-1}). A plot of q_e versus ln c_e is used to determine the constants K_1 and K_2 (Figure 7c). The value of K_1 and K_2 constants and the correlation coefficients for Tempkin isotherm are presented in Table 2.

Dubinin−Radushkevich (DR) Isotherm. Another equation used in the analysis of isotherms was proposed by Dubinin and Radushkevich. The DR model was applied to estimate the porosity apparent free energy and characteristic of adsorption. The DR isotherm does not assume a homogeneous surface or constant adsorption potential. The linear form of the DR isotherm can be given as:

$$\ln q_e = \ln Q_m - \beta\varepsilon^2 \tag{12}$$

where Q_m is the theoretical monolayer saturation capacity (mg·g^{-1}), β is the DR model constant (mol^2·kJ^{-2}), and ε is the Polanyi potential equal to $\varepsilon = RT \ln[1 + (1/C_e)]$. R is the universal gas constant in J·mol^{-1}·K^{-1}, and T is the temperature in Kelvin. With the help of this isotherm, the mean of adsorption energy E is calculated using the following relation:

$$E = \frac{1}{\sqrt{-2\beta}} \tag{13}$$

The mean of adsorption energy (E) gives information about the chemical and physical capture of adsorption.[21−24] The plot of ln q_e versus ε^2 is presented in Figure 7d. The constants obtained for the DR isotherm are shown in Table 2.

Thermodynamic Study. The thermodynamic parameters for the adsorption of BCG by an adsorbent such as enthalpy change (ΔH), the Gibbs free energy change (ΔG), and entropy change (ΔS) were determined by using the following equations.

$$\ln K_c = \frac{\Delta S}{R} - \frac{\Delta H}{RT} \qquad \frac{q_t}{C_t} = K_c \tag{14}$$

The plot of ln k_c versus $1/T$ is used to determine ΔS and ΔH and $\Delta G = \Delta H - T\Delta S$.[25] The negative free energy values indicate the feasibility of the process and its spontaneous nature. The positive values of enthalpy change (ΔH) for the processes further confirm the endothermic nature of the processes, whereas the positive values of entropy change (ΔS) reflect good affinity of the dye toward the adsorbent.[11] The data and plot ln k_c versus $1/T$ are presented in Table 3 and Figure 8. To further support the assertion that (physical or chemical) adsorption is the predominant mechanism, the value of activation energy (E_a) and sticking probability (s^*) were estimated from the experimental data. They were calculated using a modified Arrhenius type equation related to surface coverage as follows:

$$S^* = (1 - \theta)e^{-(E_a/RT)} \tag{15}$$

The sticking probability, s^*, is a function of the adsorbate/adsorbent system under investigation; its value lies in the range $0 < s^* < 1$ and is dependent on the temperature of the system. The parameter s^* indicates the measure of the potential of an adsorbate to remain on the adsorbent indefinitely.

$$\theta = \left[1 - \frac{C_e}{C_o}\right] \tag{16}$$

The activation energy and sticking probability were estimated from a plot of $\ln(1 - \theta)$ versus $1/T$ (Figure 9); the positive values of E_a indicate the endothermic nature of the adsorption process. Table 3 indicates that the probability of BCG dye to stick on the surface of ZPN is very high as $s^* \ll 1$; these values confirm that the adsorption process is physisorption.[24−27]

$$\ln(1 - \theta) = \ln S^* + \frac{E_a}{RT} \tag{17}$$

Removal of BCG from Real Samples (Bashar River, Tap Water, and Mineral Water). The removal procedure was successfully applied to the removal of BCG spiked to Bashar River, tap, and mineral waters. As the results in Table 4 show, quantitative removal (> 95 %) is obtained in all samples.

Comparison of ZPN Performance with the Other Adsorbents. As mentioned above, ZPN is a natural adsorbent with the special characteristics such as large area, desired pores, and short contact time. In Table 5, the performance of adsorbent used in proposed method has been compared with other adsorbents including natural and synthetic ones. As is seen, the adsorption capacity and contact time for ZPN in comparison with most of the natural and synthetic adsorbents are preferable. Also, in comparison with the others such as activated-charcoal, zeolite, cane pith, and silica gel, it is preferable viewing contact time but relatively poor in terms of adsorption capacity.

CONCLUSION

The following conclusion may be drawn from the present investigation.

ZPN, with the special characteristics such as availability, inexpensiveness, large area, and the desired pores, is used for the removal of dyes such as BCG from its aqueous solution. The experimental data were in line with the Tempkin, Freundlich, and Langmuir adsorption isotherms. The surface morphology studies using SEM proves that it contains more pores that lead to develop more adsorption sites. The adsorption process is dependent on pH and temperature and follows a pseudosecond-order kinetics rate model. The values of ΔH, ΔS, and ΔG results show that the adsorbent employed has considerable potential as an adsorbent for the removal of dye.

AUTHOR INFORMATION

Corresponding Author

*E-mail address: ashokrollahi@mail.yu.ac.ir.

REFERENCES

(1) Malik, P. K. Use of activated carbon prepared from sawdust and rice-husk for adsorption of acid dyes: a case study of acid yellow 36. *Dyes Pigm.* **2002**, *56*, 239–249.

(2) Faraji, M.; Yamini, Y.; Tahmasebi, E.; Saleh, A.; Nourmohammadian, F. Cetyltrimethylammonium bromide- coated magnetite nanoparticles as highly efficient adsorbent for rapid removal for reactive dyes from the textile companies wastewaters. *J. Iran Chem. Soc.* **2010**, *7*, 130–144.

(3) Yuzhu, F.; Viraraghavan, T. Removal of congo red from an aqueous solution by fungus aspergillus niger. *Adv. Environ. Res.* **2002**, *7*, 239–247.

(4) Purkait, M. K.; Dasgupta, S. Adsorption of eosin dye on activated carbon and its surfactant based desorption. *J. Environ. Manage.* **2005**, *76*, 135–142.

(5) Lau, K. T.; Brady, S.; Cleary, J.; Diamond, D. Integration of analytical measurements and wireless communications—Current issues and future strategies. *Talanta* **2008**, *75*, 606.

(6) Qadri, S.; Ganoe, A.; Haik, Y. Removal and recovery of acridine orange from solution by use of magnetic nanoparticles. *J. Hazard. Mater.* **2009**, *169*, 318–323.

(7) Murugan, T.; Ganapathi, A.; Valliappan, R. Removal of dyes from aqueous solution by adsorption on biomass of mango leaves. *E. J. Chem.* **2010**, *7*, 669–676.

(8) Ansari, R.; Mosayebzade, Z. Removal of basic dye methylene blue from aqueous solution using sawdust coated with polypyrrole. *J. Iran Chem. Soc.* **2010**, *7*, 339–350.

(9) Lin, J. X.; Zhan, S. L.; Fang, M. H.; Qian, X. Q.; Yang, H. Adsorption of basic dye from aqueous solution onto fly ash. *J. Environ. Manage.* **2008**, *87*, 193–200.

(10) Shabudeen, P. S.; Venckatesh, R.; Pattabhi, S. Preparation and utilization of kapok hull carbon for the removal of rhodamine-B from aqueous solution. *E. J. Chem.* **2006**, *3*, 83–96.

(11) Gupta, V. K.; Mittal, A.; Gajbe, V. Adsorption and desorption studies of a water soluble dye, Quinoline Yellow, using waste materials. *J. Colloid Interface Sci.* **2005**, *284*, 89–98.

(12) Ghosh, R. C. *Handbook on afforestation techniques*; Controller of Publications: Delhi, 1977.

(13) Chamargore, J. J; Bharad, J. V.; Madje, B. R.; Ubale, M. B. The removal of dye from aqueous solution by adsorption on low cost adsorbents. *E. J. Chem.* **2010**, *7*, 1003–1007.

(14) Khaled, A.; Elnemr, A.; EL-sikaily, A.; Abdelwahab, O. Removal of direct N blue-106 from artificial textile dye effluent using activated carbon from orange peel: adsorption isotherm and kinetic studies. *J. Hazard. Mater.* **2009**, *165*, 100–110.

(15) Sreelatha, G.; Ageetha, V.; Parmar, J.; Padmaja, P. Equilibrium and kinetic studies on reactive dye adsorption using palm shell powder and chitosan. *J. Chem. Eng.* **2011**, *56*, 35–42.

(16) Mittal, A.; Mittal, J.; Kurup, L.; Singh, A. K. Process development for the removal and recovery of hazardous dye erythrosine from wastewater by waste materials-bottom ash and de-oiled soya as adsorbents. *J. Hazard. Mater.* **2006**, *B138*, 95–105.

(17) Edwin Vasu, A. Studies on the removal of rhodamine b and malachite green from aqueous solutions by activated carbon. *E. J. Chem.* **2008**, *5*, 844–852.

(18) Acharya, J.; Sahu, J. N.; Mohanty, C. R.; Meikap, B. C. Removal of chromium (VI) from wastewater by activated carbon developed from Tamarind wood activated with zinc chloride. *J. Chem. Eng.* **2009**, *150*, 25–39.

(19) Arivoli, S.; Hema, M.; Karuppaiah, M.; Saravanan, S. Adsorption of chromium ion by acid activated low cost carbon-kinetic, mechanistic, thermodynamic and equilibrium studies. *E. J. Chem.* **2008**, *5*, 820–831.

(20) Mittal, A.; Kaur, D.; Mittal, J. Applicability of waste materials-bottom ash and deoiled soya-as adsorbents for the removal and recovery of a hazardous dye, brilliant green. *J. Colloid Interface Sci.* **2008**, *326*, 8–17.

(21) Mittal, A.; Mittal, J.; Malviya, A.; Gupta, V. K. Adsorptive remoal of hazardous anionic dye congo red from wastewater using waste materials and recovery by desorption. *J. Colloid Interface Sci.* **2009**, *340*, 16–26.

(22) Ferdag, C.; Necip, A.; Asim, O. Biosorption of acidic dyes from aqueous solution by paenibacillus macerans: kinetic, thermodynamic and equilibrium studies. *J. Chem. Eng.* **2009**, *150*, 122–130.

(23) Shokoohi, R.; Vatanpoor, V.; Zarrabi, M.; Vatani, A. Adsorption of acid red 18 by activated carbon from poplar wood-A kinetic and equilibrium study. *E. J. Chem.* **2010**, *7*, 65–72.

(24) Nevine Kamel, A. Removal of direct blue-106 dye from aqueous solution using new activated carbons developed from pomegranate peel: Adsorption equilibrium and kinetics. *J. Hazard. Mater.* **2009**, *165*, 52–62.

(25) Mittal, A.; Gajbe, V.; Mittal, J. Removal and recovery of hazardous tripphenylmethane dye, methyl violet through adsorption over granulated waste materials. *J. Hazard. Mater.* **2008**, *150*, 364–375.

(26) Nevine, K. A. Removal of reactive dye from aqueous solution by adsorption onto activated carbons prepared from sugarcane bagasse pith. *Desalination* **2008**, *223*, 152–161.

(27) Rajeev, J.; Gupta., V. K.; Shalini, S. Adsorption and desorption studies on hazardous dye naphthol yellow S. *J. Hazard. Mater.* **2010**, *182*, 749–756.

(28) Sujatha, M.; Geetha, A.; Sivakumar, P.; Palanisamy, P. N. Orthophosphoric acid activated babul seed carbon as an adsorbent for the removal of methylene blue. *E. J. Chem.* **2008**, *5*, 742–753.

(29) Moghimi, A.; Sheshmani, S.; Shokrollahi, A.; Shamsipur, M.; Kickelbik, G.; Aghabozorg, H. Crystal structures and solution studies of two novel Zinc(II) complexes of a proton transfer compound obtained from 2,6-pyridinedicarboxylic acid and 1,10-phenanthroline: Observation of strong intermolecular hydrogen bond. *Anorg. Z. Allg. Chem.* **2005**, *631*, 160.

(30) Aghabozorg, H.; Ramezanipour, F.; Soleimannejad, J.; Sharif, M. A.; Shokrollahi, A.; Shamsipur, M.; Moghimi, A.; Attar Gharamaleki, J.; Lippolis, V.; Blake, A. J. Different Complexation Behavior of a Proton Transfer Compound Obtained from Pyridine-2,6-dicar boxylic Acid and Creatinine with Tl(I), Cu(II), Fe(III) and Bi(III): Synthesis, Characterization, Crystal Structure and Solution Studies. *Pol. J. Chem.* **2008**, *82*, 487–507.

(31) Aghajani, Z.; Aghabozorg, H.; Sadr-Khanlou, E.; Shokrollahi, A.; Derki, S.; Shamsipur, M. Chromium (III) and Calcium(II) Complexes Obtained from Dipicolinic Acid: Synthesis, Characterization, X-Ray Crystal Structure and Solution Studies. *J. Iran Chem. Soc.* **2009**, *6*, 373–385.

(32) Shokrollahi, A.; Ghaedi, M.; Rajabi, H. R.; Niband, M. S. Potentiometric study of binary complexes of methyl 2-pyridyl ketone oxime, phenyl 2-pyridyl ketone oxime and diacetyl monooxime with some transition and heavy metal ions in aqueous solution. *Spectrochim. Acta, Part A* **2008**, *71*, 655–662.

(33) Martell, A. E.; Motekaitis, R. J. *Determination and Use of Stability Constants*, 2nd ed.; VCH: New York, 1992.

(34) Alderighi, L.; Gans, P.; Ienco, A.; Peters, D.; Sabantini, A.; Vacca, A. Hyperquad simulation and speciation (HySS): a utility program for the investigation of equilibria involving soluble and partially soluble species. *Coord. Chem. Rev.* **1999**, *184*, 311–318.

(35) Choy, K. H.; McKay, G.; Porter, J. F. Sorption of acid dyes from effluents using activated carbon. *Resour. Conserv. Recycl.* **1999**, *27*, 57–71.

(36) Jain, A. K.; Gupta, V. K.; Bhatnagar, A.; Suhas Utilization of industrial waste products as adsorbents for the removal of dyes. *J. Hazard. Mater.* **2003**, *101*, 31–42.

(37) Meshko, V.; Markovska, L.; Mincheva, M.; Rodrigues, A. E. Adsorption of basic dyes on granular activated carbon and natural zeolite. *Water Res.* **2001**, *35*, 3357–3366.

(38) Gupta, G. S.; Shukla, S. P. An inexpensive adsorption technique for the treatment of carpet effluents by low cost materials. *Adsorpt. Sci. Technol.* **1996**, *13*, 15–26.

(39) Khattri, S. D.; Singh, M. K. Colour removal from dye wastewater using sugar cane dust as an adsorbent. *Adsorpt. Sci. Technol.* **1999**, *17*, 269–282.

(40) Juang, R. S.; Tseng, R. L.; Wu, F. C. Role of microporosity of activated carbons on their adsorption abilities for phenols and dyes. *Adsorption* **2001**, *7*, 65–72.

(41) Rabia, R.; Tariq, M.; Jamil, A.; Muhammad, S.; Umer, S.; Waheed, Z.; Furqan, A. Removal of Alizarin Red S (Dye) from Aqueous Media by using Alumina as an Adsorbent. *J. Chem. Soc. Pak.* **2011**, 33.

(42) Koner, S.; Kumar Saha, B.; Kumar, R.; Adak, A. Adsorption kinetics and mechanism of methyl orange dye on modified silica gel factory waste. *Int. J. Curr. Res.* **2011**, *33*, 128–133.